Link Dynamics and Protocol Design in a Multihop Mobile Environment

Prince Samar and Stephen B. Wicker

Abstract—A multihop ad hoc network with mobile elements is considered. A model is created and analytic expressions derived to characterize the statistics for link lifetime, new link interarrival time, link breakage interarrival time, and link change interarrival time. Applications of these expressions to protocol design are discussed. As an example application, the link model is used to find an optimal balance between reactive and proactive routing strategies. It is shown that, when control traffic generated through proactive route updating is matched to link lifetimes, control traffic is significantly reduced while the goodput and delay benefits of the proactive approach are retained.

Index Terms—Ad hoc networks, link dynamics, mobility, proactive routing, protocol design, sensor networks, proactive updating, wireless link.

1 Introduction

Many existing and proposed wireless ad hoc/sensor networks have mobile elements. In remote sensing applications, for example, Unmanned Aerial Vehicles (UAVs) are often used to retrieve information through overflights of fields of static sensors. In other applications, sensors or communication nodes may be mounted on moving ground-based objects, such as automobiles, tanks, or small children. In all of these examples, the quality of the communication links formed between network entities will vary over time. In extreme cases, as may occur with very large networks of severely energy-constrained nodes, communication links will have a limited overall lifetime, coming into and passing out of existence as nodes move toward and away from each other. In such cases, local and global network connectivity is time varying, which may significantly affect the performance of network control algorithms.

In this paper, we explore the manner in which mobility affects network communication by studying the behavior of communication links in a systematic manner. The objective of the study is a deeper understanding of link dynamics and its dependence on various network characteristics. The intuition developed in the process is then applied to the design of efficient protocols for mobile multihop networks.

We begin by establishing an analytical framework for communication links when one or both endpoints are moving. We derive formal expressions for a number of link properties. Second, we show how the resulting framework can be applied to the analysis and optimization of existing protocols, as well as to the design of new, more efficient control protocols. A number of applications of the framework to medium access control, routing, transport control, topology control, and Quality of Service (QoS) provisions are considered. Finally, we explore a detailed application of our link model, showing how it can be used in the design of an efficient updating strategy for proactive routing protocols. Using simulations, we show that the proposed strategy reduces control traffic by as much as a factor of two while retaining the benefits of the proactive approach.

The organization of the rest of the paper is as follows: In Section 2, we discuss related work on the effects of mobility on link characteristics in an ad hoc or sensor network. We derive an analytical framework to study link dynamics in Section 3. In Section 4, the derived expressions are confirmed through simulation results. A number of applications of the developed framework are discussed in Section 5. In Section 6, we design and evaluate an updating strategy for proactive routing protocols. Finally, Section 7 concludes the paper.

2 Related Work

In the literature, simulation has been the primary tool utilized to characterize and evaluate link dynamics in ad hoc and sensor networks. Some efforts have been directed at designing routing schemes that rely on the identification of stable links in the network. Nodes make online measurements in order to categorize stable links, which are then preferentially used for routing. In Associativity-Based Routing (ABR) [34], nodes generate a beacon regularly to advertise their presence to their neighbors. A count of the number of beacons received from each neighbor is maintained in the form of associativity "ticks," which indicate the stability of a particular link. In Signal Strength-based Adaptive Routing (SSA) [7], received signal strength is also used in addition to location stability to quantify the reliability of a link. A routing metric is employed to select paths that consist of links with relatively strong signal strength and having an age above a certain

- *P. Samar is with Airvana Inc., Chelmsford, MA 01824. E-mail: prince.samar@gmail.com.*
- *S.B. Wicker is with the School of Electrical and Computer Engineering, Cornell University, 386 Rhodes Hall, Ithaca, NY 14853. E-mail: wicker@ece.cornell.edu.*

Manuscript received 1 Mar. 2005; revised 24 July 2005; accepted 3 Aug. 2005; published online 17 July 2006.
For information on obtaining reprints of this article, please send e-mail to: tmc@computer.org, and reference IEEECS Log Number TMC-0048-0305.

threshold. Both of these approaches suffer from the fact that a link which is deemed stable based on past or current measurements may soon become unreliable as compared to those currently categorized as unstable, due to the dynamic nature of mobile environments.

The Route-Lifetime Assessment–Based Routing (RABR) [1] uses an affinity parameter based on the measured rate of change of signal strength averaged over the last few samples in order to estimate the lifetime of a link. A metric combining the affinity parameter and the number of links in the route is then used to select routes for TCP traffic. However, shadow and multipath fading experienced by the received signal make the estimation of link lifetime error-prone. Su et al. [33] instead rely on information provided by a Global Positioning System (GPS) about the current positions and velocities of two neighboring nodes to predict the expiration time of a link.

Empirical distributions of link lifetime and residual link lifetime have been presented in [9] for different simulation parameters. Based on these results, two link stability metrics are proposed to categorize stable links. Sadagopan et al. [29] also use simulations to study the probability densities of link lifetime and route lifetime for some mobility models. The *edge effect* was identified in [20], which is the tendency of shortest routes in high density wireless networks to be unstable. This is because such routes are usually composed of nodes that lie at the edges of each others' transmission ranges so that a relatively small movement of any node in the route is sufficient to break it. The estimated stability of links has been used as the basis of route caching strategies for reactive routing protocols [15].

Analytical study of link characteristics in a mobile network has been limited. Though a number of mobility models have been proposed and used in the literature [5], none of them is satisfactory for representing node mobility in general. The commonly used *random waypoint* mobility model has been studied in [3] and [4] to investigate certain mobility properties like transition length and time of a mobile node between two waypoints, the direction angle at the beginning of a movement transition, and the spatial distribution of nodes. It has been found that the random waypoint model leads to nonuniform spatial distribution of nodes such that there is a higher concentration of nodes toward the center of the network region than close to the boundaries. Further, the model could lead to unreliable results as it fails to give a steady state, with the average nodal speed consistently decreasing over time [39].

The expected link lifetime of a node is examined for some simple mobility scenarios in [36]. It is shown that the expected link lifetime under Brownian motion is infinite, while, under deterministic mobility, it can be found explicitly, given the various parameters.

A random mobility model has been developed in [21], which is then used to quantify the probability that a link will be available between two nodes after an interval of duration t, given that the link exists between them at time t_0. This probability is then used to evaluate the availability of a path after a duration t, assuming independent link failures. This forms the basis of a dynamic clustering algorithm such that more reliable members get selected to form the cluster. However, selection of paths for routing using this criteria may not be practical as the model considers a link to be available at time $t_0 + t$ even when it undergoes failure during one or more intervals between t_0 and $t_0 + t$. When a link of a route actively being used breaks, it may be necessary to find an alternate route immediately, instead of just waiting indefinitely for the link to become available again. Jiang et al. [16] try to overcome this drawback by estimating the probability that a link between two nodes will be continuously available for a period T_p, where T_p is predicted based on the nodes' current movements.

Approximations to the distribution of link distances within a rectangular region are presented in [22], assuming that the x and y node coordinates follow independent continuous spatial distributions. In [35], the distribution of the lifetime of a given route is determined using a random walk model for node mobility. However, it is assumed that the velocity of all the nodes is the same and remains fixed at all times. Also, space (i.e., the network region) as well as time is discretized for the analysis.

Although these works shed some light, many important issues related to the behavior of links remain largely unexplored. In this paper, we develop an analytical framework in order to investigate link dynamics. To the best of the authors' knowledge, such a study at this level has not been done before. As will be seen later, the developed framework can be instrumental in the design and analysis of networking algorithms.

3 Link Dynamics

In this section, we develop a framework for analyzing the dynamics of communication links in a mobile multihop network. A number of analytical expressions are derived to characterize link behavior.

We begin with the following assumptions and arguments for their being reasonable:

1. A node has a bidirectional communication link with any other node that is within a distance of R meters. The link breaks if the distance between the nodes becomes greater than R.
2. A node in the network moves with a constant velocity which is uniformly distributed between a meters/second and b meters/second.
3. The direction of a node's velocity is uniformly distributed between 0 and 2π.
4. A node's speed, its direction of motion, and its location are mutually independent.
5. The initial locations of nodes in the network are modeled by a two-dimensional *Poisson Process* with intensity σ such that, for a network region $\mathbf{D}$ with an area A, the probability that $\mathbf{D}$ contains k nodes is given by

$$Prob(k\ nodes\ in\ \mathbf{D}) = \frac{(\sigma A)^k e^{-\sigma A}}{k!}. \qquad (1)$$

Assumption 1 implies that the Signal to Interference Ratio (SIR) remains high up to a certain distance R from the

transmitter, enabling a nearly perfect estimation of the transmitted signal. However, SIR drops beyond this distance, rapidly increasing the Bit Error Rate (BER) to unacceptable levels. Such rapid deterioration of performance is typical of channels encoded with powerful error control codes (witness the standard "waterfall" curves of Reed-Solomon and turbo-coded channels [38]). Though the shadowing and multipath fading experienced by the received signal may make the actual transmission zone asymmetrical, the above is a fair approximation if all the nodes in the network use the same transmission power.

Assumption 2 models a mobile environment where nodes are moving around with different velocities that are uniformly distributed between two limits. This high mobility model is chosen as it is challenging for network communication and, thus, can facilitate finding "worst-case" bounds on the link properties for a general scenario. It is to be noted that the degree of mobility in a given application can be taken into account by appropriately choosing the two parameters, a and b.

Assumptions 2-5 characterize the aggregate behavior of nodes in a large network. Due to the large number of independent nodes operating in an ad hoc fashion, any correlation between nodes can be assumed to be insignificant. Although it is possible that some nodes may share similar objectives and may move together, a large enough population of autonomous nodes can be expected in the network so that the composite effect can be modeled by a random process.

Note that Assumption 5 indicates the location distribution of nodes in the network at the start and, as a consequence, at any later point of time. This follows from *Bartlett's Theorem* [18] as the node velocities are mutually independent. Poisson processes model "total randomness," thus reflecting the randomness shown by the aggregate behavior of nodes in a large network. This assumption is frequently used to model the location of nodes in an ad hoc or cellular network. Using (1), it is easy to see that the expected number of nodes in $\mathbf{D}$ is equal to σA. Thus, σ represents the average density of nodes in the network.

3.1 Expected Link Lifetime

Fig. 1 shows the transmission zone of a node (say node 1), which is a circle of radius R centered at the node. The figure shows the trajectory of another node (say node 2) entering the transmission zone of node 1 at A, traveling along AB, and exiting the transmission zone at B.

With respect to a stationary Cartesian coordinate system with orthogonal unit vectors $\hat{i}$ and $\hat{j}$ along the X and Y axes, respectively, let the velocity of node 1 be $\vec{v}_1 = v_1\hat{i}$ and the velocity of node 2, which makes an angle θ with the positive X axis, be $\vec{v}_2 = v_2\cos\theta\hat{i} + v_2\sin\theta\hat{j}$. Hence, the relative velocity of node 2 with respect to node 1 is

$$\vec{v} \triangleq \vec{v}_{21} = \vec{v}_2 - \vec{v}_1 = (v_2\cos\theta - v_1)\hat{i} + v_2\sin\theta\hat{j}. \tag{2}$$

Consider a Cartesian coordinate system $X'Y'$ fixed on node 1 such that the X' and Y' axes are parallel to $\hat{i}$ and $\hat{j}$, respectively, as shown in Fig. 1. The magnitude of node 2's velocity in this coordinate system is

$$v \triangleq |\vec{v}| = \sqrt{v_1^2 + v_2^2 - 2v_1v_2\cos\theta} \tag{3}$$

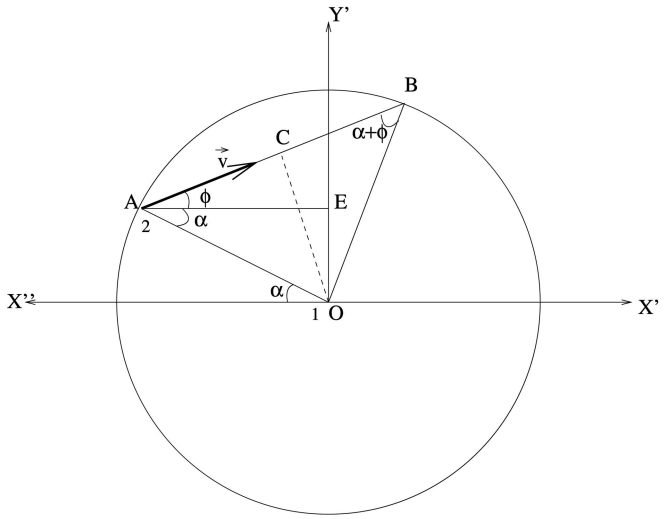

Fig. 1. The transmission zone of node 1 at O with node 2 entering the zone at A and exiting at B.

and its direction of motion in this coordinate system, as indicated in Fig. 1, is

$$\phi \triangleq \angle\vec{v} = \tan^{-1}\Big(\frac{\sin\theta}{\cos\theta - v_1/v_2}\Big). \tag{4}$$

Let node 2's point of entry A in node 1's transmission zone be defined by an angle α, measured clockwise from OX''. Thus, point A has coordinates $(-R\cos\alpha, R\sin\alpha)$ in the $X'Y'$ coordinate system. In Fig. 1, $OA = OB = R$. AB makes an angle ϕ with the horizontal, which is the direction of the relative velocity of node 2. Line OC is perpendicular to AB. As OAB makes an isosceles triangle, $\angle OAB = \angle OBA = \alpha + \phi$. Therefore, $AC = BC = R\cos(\alpha + \phi)$. As θ and ϕ can have any value between 0 and 2π, the distance d_{link} that node 2 travels inside node 1's zone is

$$d_{link} = |2R\cos(\alpha + \phi)| = 2R|\cos(\alpha + \phi)|. \tag{5}$$

Hence, the time that node 2 spends inside node 1's zone, which is equal to the time for which the link between node 1 and node 2 remains active, is

$$\begin{aligned} t_{link} &= \frac{d_{link}}{|\vec{v}|} \\ &= \frac{2R|\cos(\alpha + \phi)|}{v}. \end{aligned} \tag{6}$$

The mean link lifetime of node 1 as a function of its velocity v_1 can be calculated as the expectation of t_{link} over v, ϕ, α:

$$\bar{T}_{link}(v_1) = E_{v\phi\alpha}\big[t_{link}(v, \phi, \alpha)\big]. \tag{7}$$

Let the joint probability density function of v, ϕ, α for nodes that enter the zone be $f_{v\phi\alpha}(v, \phi, \alpha)$. It can be expressed as

$$f_{v\phi\alpha}(v, \phi, \alpha) = f_{\alpha|v\phi}(\alpha|v, \phi)f_{v\phi}(v, \phi), \tag{8}$$

where $f_{\alpha|v\phi}(\alpha|v, \phi)$ is the conditional probability density of α given the relative velocity $\vec{v}$ and $f_{v\phi}(v, \phi)$ is the joint probability density of the magnitude v and phase ϕ of $\vec{v}$. Expressions for these probability density functions are derived in the Appendix.

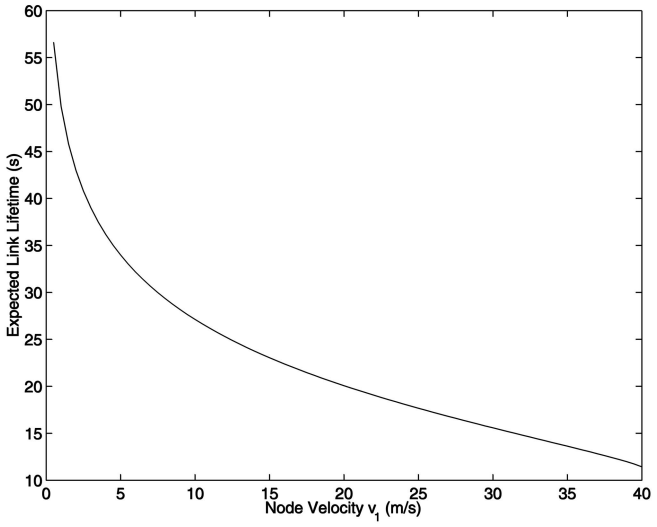

Fig. 2. Expected Link Lifetime of a node as a function of its velocity, where $a = 0m/s$, $b = 40m/s$, and $R = 250m$.

Thus, the expected link lifetime as a function of node velocity v_1 can be evaluated as

$$\bar{T}_{link}(v_1) = \int_0^{\infty} \int_{-\pi}^{\pi} \int_{-\pi}^{\pi} t_{link} f_{v\phi\alpha}(v, \phi, \alpha) d\alpha d\phi dv. \quad (9)$$

Using (6) and (56) to simplify (9), we get

$$\bar{T}_{link}(v_1) = \frac{R}{2(b-a)} \left(\int_0^{\pi} \log \left| \frac{b + \sqrt{b^2 - v_1^2 \sin^2 \phi}}{v_1 + v_1 \cos \phi} \right| d\phi - \int_{\phi_0}^{\pi} \log \left| \frac{a + \sqrt{a^2 - v_1^2 \sin^2 \phi}}{a - \sqrt{a^2 - v_1^2 \sin^2 \phi}} \right| d\phi \right), \quad (10)$$

where $\phi_0 = \pi - sin^{-1}(\frac{a}{v_1})$. For the case when the lower bound on the node velocity $a = 0$, the above expression reduces to

$$\bar{T}_{link}(v_1) = \frac{R}{2b} \left(\int_0^{\pi} \log \left| \frac{b + \sqrt{b^2 - v_1^2 \sin^2 \phi}}{v_1 + v_1 \cos \phi} \right| d\phi \right). \quad (11)$$

Equation (10) cannot be further integrated into an explicit function. However, it can be numerically integrated to give the expected link lifetime for the chosen distribution of mobility in the network.

Fig. 2 plots the expected link lifetime for a node as a function of its velocity. The velocity of the nodes in the network is assumed to be uniformly distributed between [0, 40] meters/second. As can be observed from the plot, the expected link lifetime for a node decreases rapidly as its velocity is increased. As an illustration, links last almost three times longer, on average, for a node moving with a velocity of 5 meters/second as compared to a node moving with a velocity of 40 meters/second. Also, as can be seen from (10), the expected link lifetime is directly proportional to the transmission radius R of a node.

It is to be noted that Assumption 5 was not needed for determining the expected link lifetime and, thus, the derived expression is independent of the density of nodes in the network. This is because $\bar{T}_{link}(v_1)$ is averaged over link lifetimes corresponding to the range of velocities present in the network weighted by their probability density, without regard to how many or how often these links are formed.

3.2 Link Lifetime Distribution

For a particular node moving with a velocity v_1, the cumulative distribution function (CDF) of the link lifetime is defined as

$$F_{link}^{v_1}(t) = Prob\{t_{link} \leq t\}. \quad (12)$$

Clearly, $F_{link}^{v_1}(t) = 0$ for $t < 0$. For $t \geq 0$, we have

$$F_{link}^{v_1}(t) = Prob\Big\{ \frac{2R|\cos(\alpha + \phi)|}{v} \leq t \Big\} = 1 - Prob\Big\{ |\cos(\alpha + \phi)| > \frac{vt}{2R} \Big\}. \quad (13)$$

Now,

$$Prob\Big\{ |\cos(\alpha + \phi)| > \frac{vt}{2R} \Big\} = \int_{\phi=-\pi}^{\pi} \int_{v=0}^{\frac{2R}{t}} \int_{\alpha=-cos^{-1}(\frac{vt}{2R})-\phi}^{cos^{-1}(\frac{vt}{2R})-\phi} f_{v\phi\alpha}(v, \phi, \alpha) d\alpha dv d\phi. \quad (14)$$

Using the expression of $f_{v\phi\alpha}(v, \phi, \alpha)$ from (56) and (14), (13) can be simplified to give the link lifetime CDF for a node moving with velocity v_1:

$$F_{link}^{v_1}(t) = 1 - \frac{1}{\pi(b-a)} \int_0^{\pi} \int_0^{\frac{2R}{t}} v \sqrt{1 - \Big(\frac{vt}{2R}\Big)^2} g(v, \phi, v_1) dv d\phi, \quad (15)$$

where

$$g(v, \phi, v_1) = \frac{u\big(h(v, \phi, v_1) - a\big) - u\big(h(v, \phi, v_1) - b\big)}{h(v, \phi, v_1)}, \quad (16)$$

$$h(v, \phi, v_1) = \sqrt{v^2 + v_1^2 + 2vv_1 \cos \phi}, \quad (17)$$

and $u(\cdot)$ is the standard unit step function.

No closed-form solution for the integrals in (15) is known (by the authors). However, (15) can be numerically integrated to give the cumulative distribution function of the link lifetime for a node moving with velocity v_1. Fig. 3a plots the link lifetime CDF for different node velocities v_1, where $a = 0\ meters/second$, $b = 40\ meters/second$, and $R = 250\ meters$.

The probability density function (PDF) $f_{link}^{v_1}(t)$ of link lifetime is found by differentiating (15) with respect to t. Fig. 3b plots the probability density function by numerically differentiating the curves in Fig. 3a. Note that, for $v_1 > 0$, the point where the PDF curve is not differentiable occurs at $t = \frac{2R}{v_1}$, which corresponds to the time taken by a node moving at velocity v_1 to pass through a transmission zone along its diameter. Also, it can be seen that the maxima of the PDF curve, which corresponds to the *mode* of the distribution, shifts toward the left as the node velocity increases.

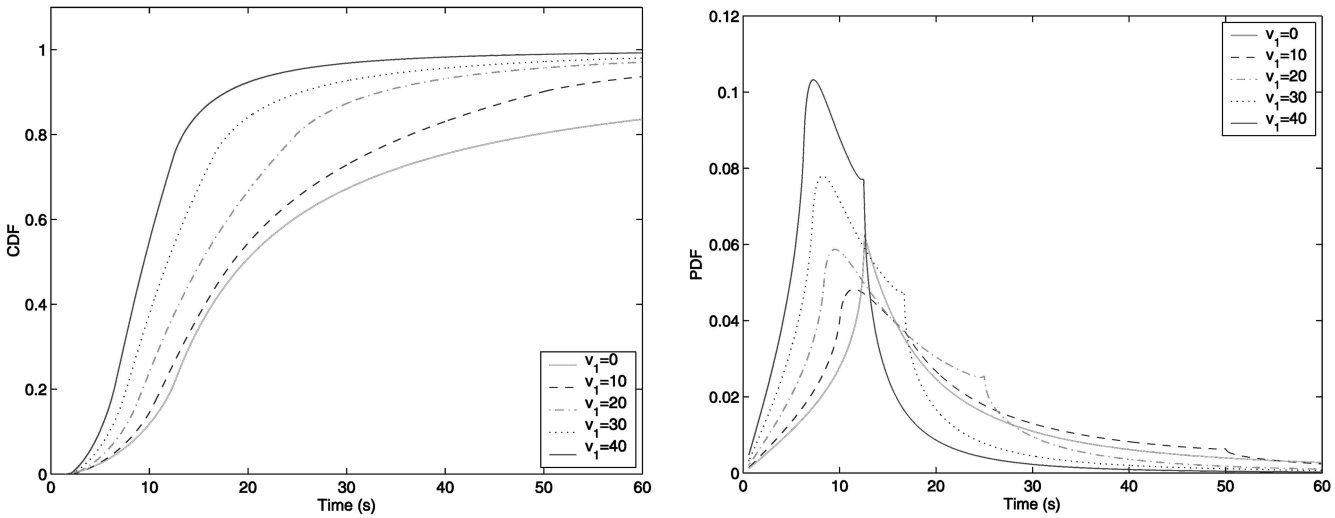

(a) (b)

Fig. 3. The (a) Cumulative Distribution Function (CDF) and (b) Probability Density Function (PDF) of the link lifetime for a node moving with velocity v_1 for $a = 0m/s$, $b = 40m/s$, and $R = 250m$.

As in Section 3.1, the derived expression does not depend on the density or location distribution of nodes in the network.

3.3 Expected New Link Arrival Rate

Consider Fig. 4, which shows the transmission zone of node 1 moving with velocity $\vec{v}_1$ with respect to the stationary coordinate system XY, as defined before. For given values of v and ϕ, any node with relative velocity $\vec{v} = v\cos\phi\hat{i} + v\sin\phi\hat{j}$ with respect to node 1 can only enter node 1's transmission zone from a point on the semicircle $\alpha \in [-(\frac{\pi}{2}+\phi), \frac{\pi}{2}-\phi]$,[1] as seen in the Appendix. Thus, a node with relative velocity $\vec{v}$ would enter the transmission zone within the next t seconds if it is currently located in the shaded region $\mathbf{D_a}$ of Fig. 4, which is the set of all points at most vt meters away measured along angle ϕ from the semicircle $\alpha \in [-(\frac{\pi}{2}+\phi), \frac{\pi}{2}-\phi]$.

The area of the shaded region $\mathbf{D_a}$ is $A = vt \cdot 2R$. Using Assumption 5, the average number of nodes in $\mathbf{D_a}$ is found to be equal to $2Rvt \cdot \sigma$. Therefore, the average number of nodes in $\mathbf{D_a}$ with velocity $\vec{v}$ is equal to $2R\sigma vt \cdot f(v,\phi)dvd\phi$. This is just the average number of nodes with velocity $\vec{v}$ entering the zone within the next t seconds. The total expected number of nodes entering the zone within the next t seconds, $\eta(v_1)$, is found by integrating this quantity over all possible values of v and ϕ:

$$\eta(v_1) = \int_{v=0}^{\infty}\int_{\phi=-\pi}^{\pi} 2R\sigma vt f(v,\phi)dvd\phi. \tag{18}$$

Thus, the expected number of nodes entering the transmission zone per second or, equivalently, the rate of new link arrivals is given by

$$\dot{\eta}(v_1) = \int_{v=0}^{\infty}\int_{\phi=-\pi}^{\pi} 2R\sigma v f(v,\phi)dvd\phi. \tag{19}$$

1. α, as defined before, is the angle measured clockwise from the negative X axis of the coordinate system fixed on node 1.

$f(v,\phi)$, the joint probability density of a node's relative velocity, is derived in (55). Thus, (19) can be simplified to give

$$\begin{aligned}\dot{\eta}(v_1) = \frac{2R\sigma}{\pi(b-a)}\Bigg[&b^2\mathcal{E}\big(\tfrac{v_1}{b}\big) - 2a^2\mathcal{E}\big(\tfrac{v_1}{a}\big) + a^2\mathcal{E}\Big(\phi_0, \tfrac{v_1}{a}\Big) \\ &+ \frac{v_1^2}{4}\int_0^{\pi} p(\phi)\log\left|\frac{b+\sqrt{b^2 - v_1^2\sin^2\phi}}{v_1 + v_1\cos\phi}\right|d\phi \\ &- \frac{v_1^2}{4}\int_{\phi_0}^{\pi} p(\phi)\log\left|\frac{a+\sqrt{a^2 - v_1^2\sin^2\phi}}{a-\sqrt{a^2 - v_1^2\sin^2\phi}}\right|d\phi\Bigg],\end{aligned} \tag{20}$$

where $\phi_0 = \pi - \sin^{-1}(\frac{a}{v_1})$, $p(\phi) = 1 + 3\cos(2\phi)$, $\mathcal{E}(\cdot)$ is the standard Complete Elliptic Integral of the Second Kind, and $\mathcal{E}(\cdot,\cdot)$ is the standard Incomplete Elliptic Integral of the Second Kind. For the case when $a = 0$, $\dot{\eta}(v_1)$ reduces to

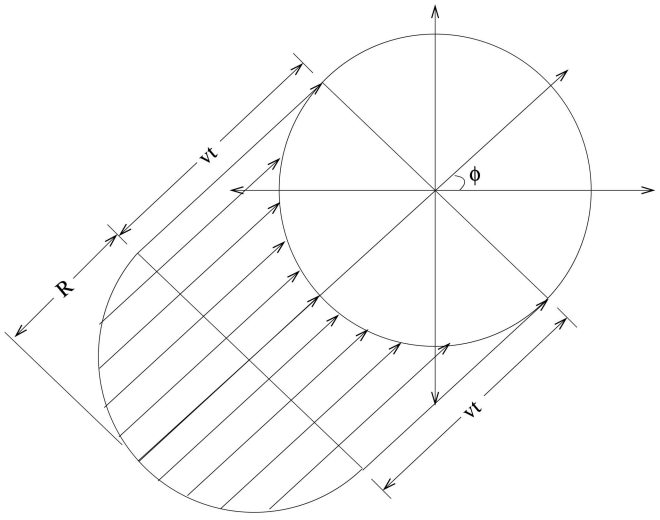

Fig. 4. Calculation of expected new link arrival rate.

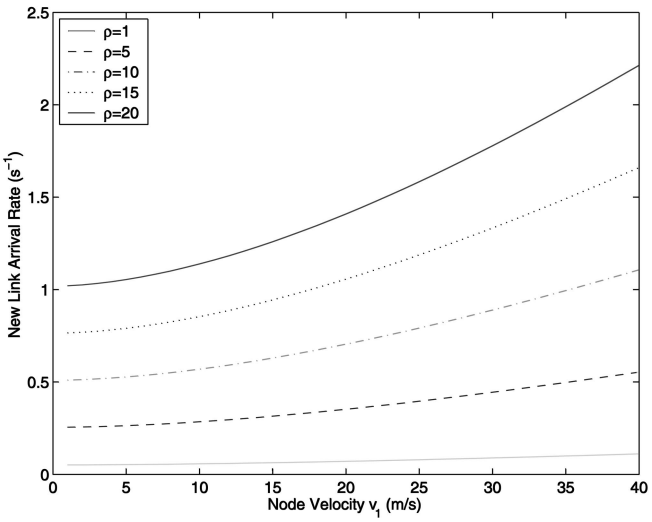

Fig. 5. Rate of new link arrivals for a node moving with velocity v_1, where $a = 0m/s$, $b = 40m/s$, $R = 250m$, and $\sigma = \frac{\rho}{\pi R^2} nodes/m^2$.

$$\dot{\eta}(v_1) = \frac{2R\sigma}{\pi b}\left[b^2\mathcal{E}\left(\frac{v_1}{b}\right) + \frac{v_1^2}{4}\int_0^{\pi} p(\phi)\log\left|\frac{b+\sqrt{b^2 - v_1^2\sin^2\phi}}{v_1 + v_1\cos\phi}\right| d\phi\right]. \tag{21}$$

In Fig. 5, we plot the expected rate of new link arrivals for a node moving with velocity v_1. While generating the curves, the values of the parameters are set to $a = 0\ meters/second$, $b = 40\ meters/second$, $R = 250\ meters$, and $\sigma = \frac{\rho}{\pi R^2}\ nodes/meter^2$. Note that ρ represents the average number of nodes within a transmission zone.

An important point to observe from (20) is that the expected rate of new link arrivals for a node is directly proportional to the average density σ of nodes in the network. It is also directly proportional to the transmission radius R of the nodes.

3.4 New Link Interarrival Time Distribution

The cumulative distribution function of new link interarrival time is defined as

$$F^{v_1}_{arrival}(t) = Prob\{link\ interarrival\ time \le t\}. \tag{22}$$

$\mathbf{D_a}$, the shaded region of Fig. 4, has an area $A = 2Rvt$. As seen in Section 3.3, a node with velocity $\vec{v} = v\cos\phi\hat{i} + v\sin\phi\hat{j}$ currently located in $\mathbf{D_a}$ will enter the transmission zone within the next t seconds. Thus, given $\vec{v}$, the probability that the link interarrival time is not more than t is equal to the probability that there exists at least one node in $\mathbf{D_a}$ with velocity $\vec{v}$. Therefore, using Assumption 5,

$$\begin{aligned} &Prob\{link\ interarrival\ time \le t|v,\phi\} \\ &= Prob\{at\ least\ 1\ node\ in\ \mathbf{D_a}|v,\phi\} = 1 - e^{-2R\sigma tv}. \end{aligned} \tag{23}$$

Hence, the cumulative distribution function of new link interarrival time can be expressed as

$$F^{v_1}_{arrival}(t) = \int\int_{v,\phi}\left(1 - e^{-2R\sigma tv}\right) f(v,\phi)dvd\phi. \tag{24}$$

Substituting for $f(v,\phi)$ from (55) in (24),

$$F^{v_1}_{arrival}(t) = 1 - \frac{1}{\pi(b-a)}\int_0^{\pi}\int_0^{\infty} ve^{-2R\sigma tv} g(v,\phi,v_1)dvd\phi, \tag{25}$$

where $g(v,\phi,v_1)$ is as defined in (16).

Fig. 6a illustrates the new link interarrival time distribution for a node moving with velocity v_1, for $a = 0\ meters/second$, $b = 40\ meters/second$, $R = 250\ meters$, and $\sigma = \frac{10}{\pi R^2}\ nodes/meter^2$. The corresponding new link interarrival time density, found by differentiating (25), is plotted in Fig. 6b for different node velocities v_1. It can be observed that the new link interarrival time PDF curves drop rapidly as time t increases. In fact, using standard curve fitting techniques, we have found that the new link interarrival time density can be very well approximated by a simple exponential function, with the Root Mean Squared Error (RMSE) for the fit being less than 0.02 for the case in Fig. 6.

3.5 Expected Link Breakage and Link Change Rates

Any change in the set of links of a node may be either due to the arrival of a new link or due to the breaking of a currently active link. Thus, the expected link change rate for a node is equal to the sum of the expected new link arrival rate and the expected link breakage rate. The expected new link arrival rate is as expressed in (20).

In order to determine the expected link breakage rate, suppose that the network is formed at time $t = 0$. Let the total number of new link arrivals for a node between $t = 0$ and $t = t_0$ be $\eta(t_0)$ and the total number of link breakages for the node during the same interval be $\mu(t_0)$. Let the number of neighbors of the node at time $t = t_0$ be $N(t_0)$. Thus,

$$\eta(t_0) - \mu(t_0) = N(t_0). \tag{26}$$

Dividing both the sides in (26) by t_0 and taking the limit as $t \to \infty$,

$$\lim_{t\to\infty}\left\{\frac{\eta(t_0)}{t_0} - \frac{\mu(t_0)}{t_0}\right\} = \lim_{t\to\infty}\frac{N(t_0)}{t_0}. \tag{27}$$

Now, $\lim_{t\to\infty}\frac{\eta(t_0)}{t_0}$ equals the expected rate of new link arrivals $\dot{\eta}$ and $\lim_{t\to\infty}\frac{\mu(t_0)}{t_0}$ equals the expected rate of link breakages $\dot{\mu}$ (assuming ergodicity). If the number of neighbors of a node is bounded,[2] $\lim_{t\to\infty}\frac{N(t_0)}{t_0} = 0$. This implies that $\dot{\mu} = \dot{\eta}$, i.e., the expected rate of link breakages is equal to the expected rate of new link arrivals. Thus, the expected link change arrival rate $\dot{\gamma}(v_1)$ for a node moving with velocity v_1 is given by

$$\begin{aligned} \dot{\gamma}(v_1) &= \dot{\eta}(v_1) + \dot{\mu}(v_1) \\ &= 2\dot{\eta}(v_1), \end{aligned} \tag{28}$$

where $\dot{\eta}(v_1)$ is as expressed in (20).

The expected link change arrival rate as a function of the node velocity v_1 is plotted in Fig. 7, where $a = 0\ meters/second$, $b = 40\ meters/second$, $R = 250\ meters$, and $\sigma = \frac{\rho}{\pi R^2}\ nodes/meter^2$. Like $\dot{\eta}(v_1)$, $\dot{\gamma}(v_1)$ is also directly proportional to the average node density σ and the node transmission radius R.

2. This is the case for any practical ad hoc or sensor network.

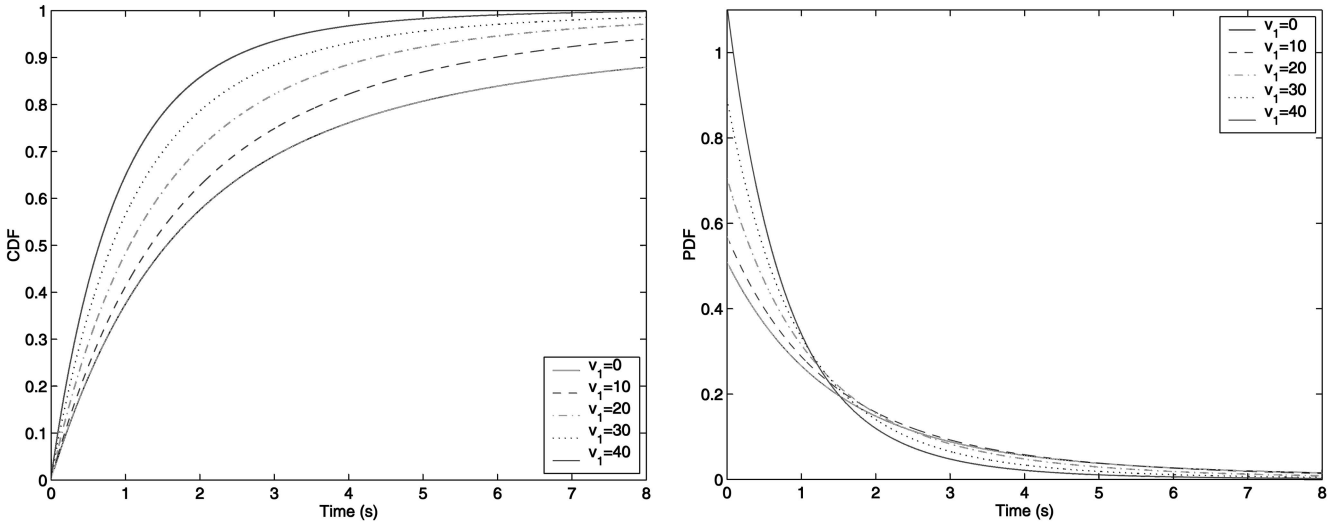

(a) (b)

Fig. 6. The (a) Cumulative Distribution Function (CDF) and (b) Probability Density Function (PDF) of new link interarrival time for a node moving with velocity v_1 for $a = 0m/s$, $b = 40m/s$, $R = 250m$, and $\sigma = \frac{10}{\pi R^2}\ nodes/m^2$.

3.6 Link Breakage Interarrival Time Distribution

In order to derive the link breakage interarrival time distribution, we proceed in a manner similar to Section 3.4. Consider Fig. 8a showing the transmission zone of node 1. The shaded region $\mathbf{D_b}$ in the figure consists of all points not more than vt meters away along angle ϕ from the semicircle $\alpha \in [\frac{\pi}{2} - \phi, \frac{3\pi}{2} - \phi]$. It is easy to see that a node moving at an angle ϕ can break a link with node 1 only by moving out of its transmission zone from a point on this semicircle. Given its relative velocity $\vec{v} = v\cos\phi\hat{i} + v\sin\phi\hat{j}$, a node will leave the transmission zone of node 1 within the next t seconds —and, thus, break the link between the two—if it is currently located in $\mathbf{D_b}$. Note that $\mathbf{D_b}$ also includes the possibility of nodes that are currently outside the transmission zone of node 1 and have yet to form a link with it.

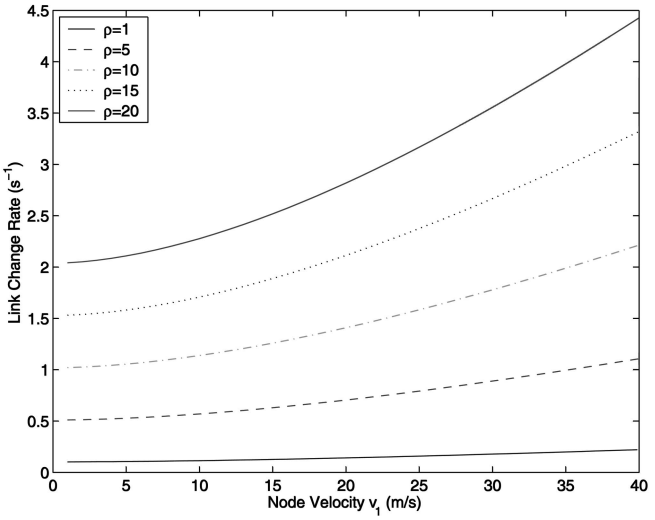

Fig. 7. Expected link change rate for a node moving with velocity v_1, where $a = 0m/s$, $b = 40m/s$, $R = 250m$, and $\sigma = \frac{\rho}{\pi R^2}\ nodes/m^2$.

The area of the shaded region $\mathbf{D_b}$ is $A = 2Rvt$. For given v and ϕ, the probability that the link breakage interarrival time is not more than t is equal to the probability that there is at least one node in $\mathbf{D_b}$ with velocity $\vec{v}$:

$$\begin{aligned} &Prob\{link\ breakage\ interarrival\ time \le t|v,\phi\} \\ &= Prob\{at\ least\ one\ node\ in\ \mathbf{D_b}|v,\phi\} = 1 - e^{-\sigma 2Rvt}. \end{aligned} \tag{29}$$

Thus, the cumulative distribution function of link breakage interarrival time is given by

$$\begin{aligned} F_{break}^{v_1}(t) &= Prob\{link\ breakage\ interarrival\ time \le t\} \\ &= \int\int_{v,\phi} \left(1 - e^{-2R\sigma tv}\right) f(v,\phi) dv d\phi. \end{aligned} \tag{30}$$

The right-hand sides of (24) and (30) are the same, implying that the distributions of link breakage interarrival time and new link interarrival time are the same and are given by (25). Note that, using a different argument, it was already shown in Section 3.5 that the expected rate of link breakages is equal to the expected rate of new link arrivals.

3.7 Link Change Interarrival Time Distribution

The creation of a new link or expiry of an old link constitutes a change in a node's local connectivity. Given its relative velocity $\vec{v} = v\cos\phi\hat{i} + v\sin\phi\hat{j}$, the existence of a node in the shaded region $\mathbf{D_a}$ of Fig. 4 will cause the formation of a new link within the next t seconds. Likewise, a node with velocity $\vec{v}$ in the shaded region $\mathbf{D_b}$ of Fig. 8a will cause the breaking of a link within the next t seconds. Fig. 8b shows the union of these two shaded regions, $\mathbf{D_c} = \mathbf{D_a} \cup \mathbf{D_b}$. Given $\vec{v}$, a node currently located in the shaded region $\mathbf{D_c}$ of Fig. 8b will cause a link change within the next t seconds.

The area A of $\mathbf{D_c}$ can be expressed as

$$A = \begin{cases} q_1(v,t) & if\ vt \le 2R \\ q_2(v,t) & if\ vt > 2R, \end{cases} \tag{31}$$

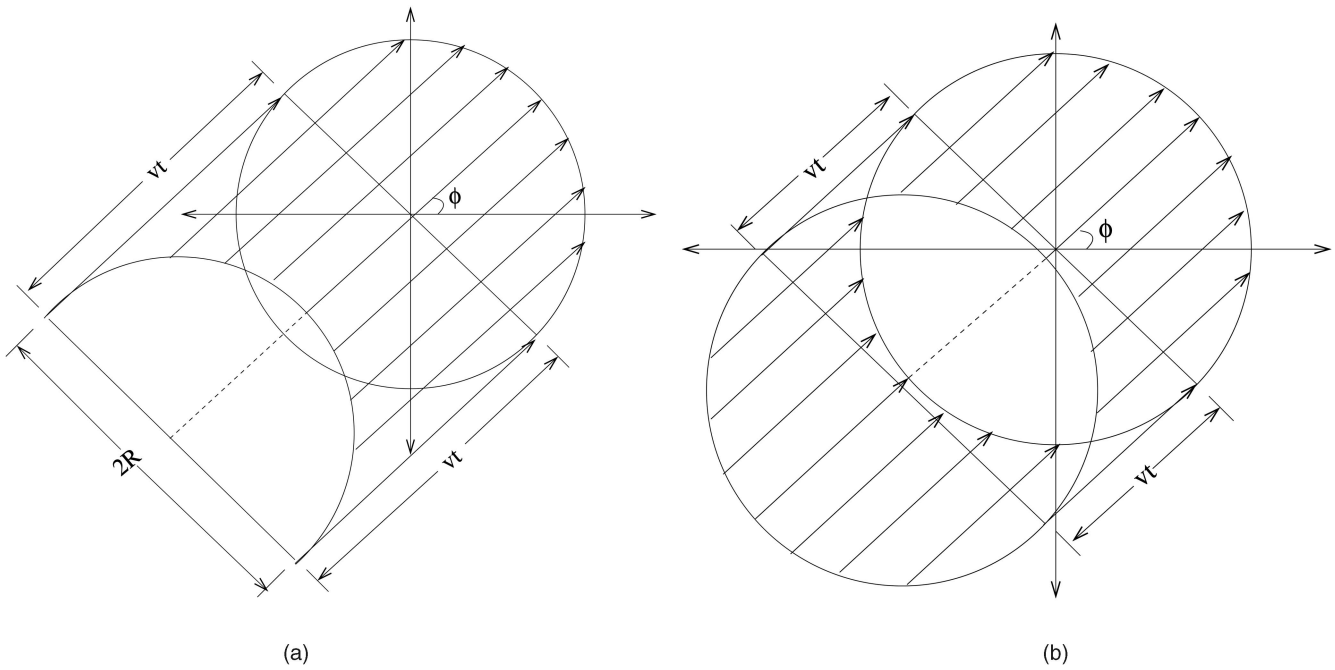

Fig. 8. Calculation of (a) link breakage interarrival time distribution and (b) link change interarrival time distribution.

where $q_1(v,t) = 2vtR + 2R^2\left(\sin^{-1}(\frac{vt}{2R}) + \frac{vt}{2R}\sqrt{1-(\frac{vt}{2R})^2}\right)$ and $q_2(v,t) = 2vtR + \pi R^2$. From Assumption 5, as the nodes are assumed to be Poisson distributed,

$$Prob\{no\ node\ in\ \mathbf{D_c}|v,\phi\} = e^{-\sigma A}. \tag{32}$$

Therefore, the link change interarrival time distribution is given by

$$\begin{aligned} F^{v_1}_{change}(t) &= Prob\{link\ change\ interarrival\ time \le t\} \\ &= 1 - \int\int_{v,\phi} e^{-\sigma A} f(v,\phi) dv d\phi. \end{aligned} \tag{33}$$

Substituting for $f(v,\phi)$ and A and simplifying,

$$\begin{aligned} F^{v_1}_{change}(t) = 1 - \frac{1}{\pi(b-a)}\Bigg(&\int_0^{\pi}\int_0^{\frac{2R}{t}} ve^{-\sigma q_1(v,t)} g(v,\phi,v_1) dv d\phi \\ &+ \int_0^{\pi}\int_{\frac{2R}{t}}^{\infty} ve^{-\sigma q_2(v,t)} g(v,\phi,v_1) dv d\phi \Bigg). \end{aligned} \tag{34}$$

It is not possible to explicitly evaluate the integrals in (34). In Fig. 9a, we plot the link change interarrival time distribution $F^{v_1}_{change}(t)$ for different node velocities v_1. $a = 0\ meters/second$, $b = 40\ meters/second$, $R = 250\ meters$, and $\sigma = \frac{10}{\pi R^2}\ nodes/meter^2$ have been used for the figure. In Fig. 9b, the corresponding link change interarrival time probability density $f^{v_1}_{change}(t)$ is plotted for the same parameter values.

It can be readily observed from the figure that the link change interarrival time density function decreases rapidly as time t increases. It is interesting to compare Fig. 6b and Fig. 9b which plot the PDFs of new link interarrival time (or link breakage interarrival time) and link change interarrival time, respectively. The curves in Fig. 9b appear to be scaled versions (by a factor of approximately 2 and then normalized) of the curves in Fig. 6b.

Although the expression for the link change interarrival time distribution in (34) looks complicated, it can be approximated by an exponential distribution function with fairly high accuracy. Using standard curve-fitting techniques, we fit the link change interarrival time density function with an exponential function of the form $f(t) = \lambda e^{-\lambda t}$. Fig. 10 plots the Root Mean Squared Error (RMSE) (also known as the standard error of regression) for this fit as a function of the node velocity for the case in Fig. 9. We see that the RMSE remains below 0.025 and is even lower at higher velocities. Similar results were obtained for other combination of parameter values, indicating a good fit.

3.8 Expected Number of Neighbors

As the locations of nodes in the network are modeled as Poisson distributed random variables with intensity σ, the expected number of nodes located in an area A is equal to σA. Consider a node located at point P_0 and an area A that includes P_0. Now, given P_0, the number of nodes in area A is independent of the node at P_0. Thus, the expected number of neighbors of a node is equal to the number of nodes in its transmission zone and is given by

$$\bar{N} = \sigma\pi R^2. \tag{35}$$

As expected, $\bar{N}$ increases with node density σ and as a square of the transmission radius R, but is independent of node mobility.

4 Comparison with Simulations

In order to validate the analytically derived expressions for the link behavior, we compare them to statistics collected from simulations of mobile networks.

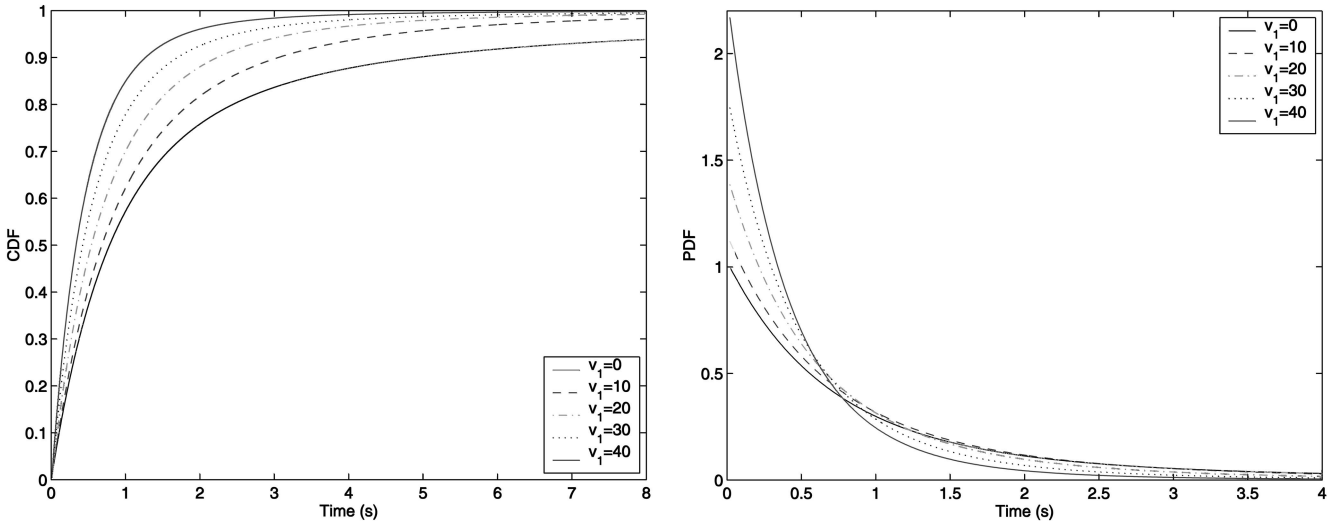

(a) (b)

Fig. 9. The (a) Cumulative Distribution Function (CDF) and (b) Probability Density Function (PDF) of link change interarrival time for a node moving with velocity v_1 for $a = 0m/s$, $b = 40m/s$, $R = 250m$, and $\sigma = \frac{10}{\pi R^2}$.

The simulation setup parameters for the results presented here are listed in Table 1. The $OPNET$™ network simulation environment is used for the simulations. The nodes in the network are initially placed randomly on the surface of a torus, constructed from a square of side $2,427\ meters$ [37]. The square size is selected such that the node density σ equals $\frac{10}{\pi R^2}\ nodes/meter^2$. The nodes move randomly on the surface of the torus and their velocity is uniformly distributed between $a = 0\ meters/second$ and $b = 40\ meters/second$.

Fig. 11, Fig. 12, and Fig. 13 compare the corresponding analytical and simulation results. As can be observed, the simulation results are in good agreement with the analytical results.

The small gap between the analytical curve and the simulation points for the expected link lifetime in Fig. 11a is attributed to the following: The finite-duration simulations involving a limited number of nodes do not represent well the possibility of the existence of pairs of nodes with very small relative velocities. Such pairs of nodes would have very large link lifetimes, the contributions of which are not appropriately captured in the simulation results. For example, a pair of nodes with velocities very close to zero can have an exceedingly large link lifetime (even though the probability of this happening is small). This explains why the average link lifetime as experienced in the simulations lies below the analytical curve, especially at lower velocities. In our simulations, we have observed that the gap reduces as the number of nodes in the network and the simulation time are increased. Further, the good match for link lifetime PDF in Fig. 11b reinforces the correctness for expected link lifetime as well.

The results for the expected link breakage rate and the link breakage interarrival time density are similar to those in Fig. 12 and are, therefore, omitted here. Simulation results for nodes moving in a rectangular region (with reflections from the edges) are also found to be in pretty good agreement with the analytical results [30].

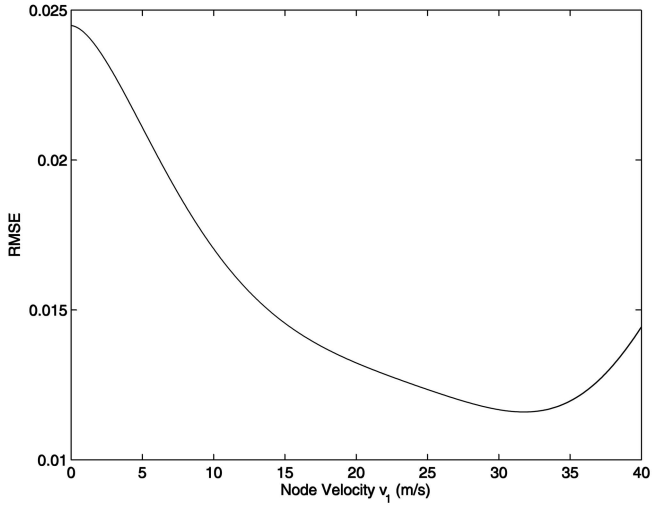

Fig. 10. Root Mean Squared Error for an exponential fit to the link change interarrival time density.

TABLE 1
Simulation Setup Parameters

Number of Nodes	300
Transmission Radius, R	250 $meters$
a	0 $meters/second$
b	40 $meters/second$
Simulation duration	90 $minutes$

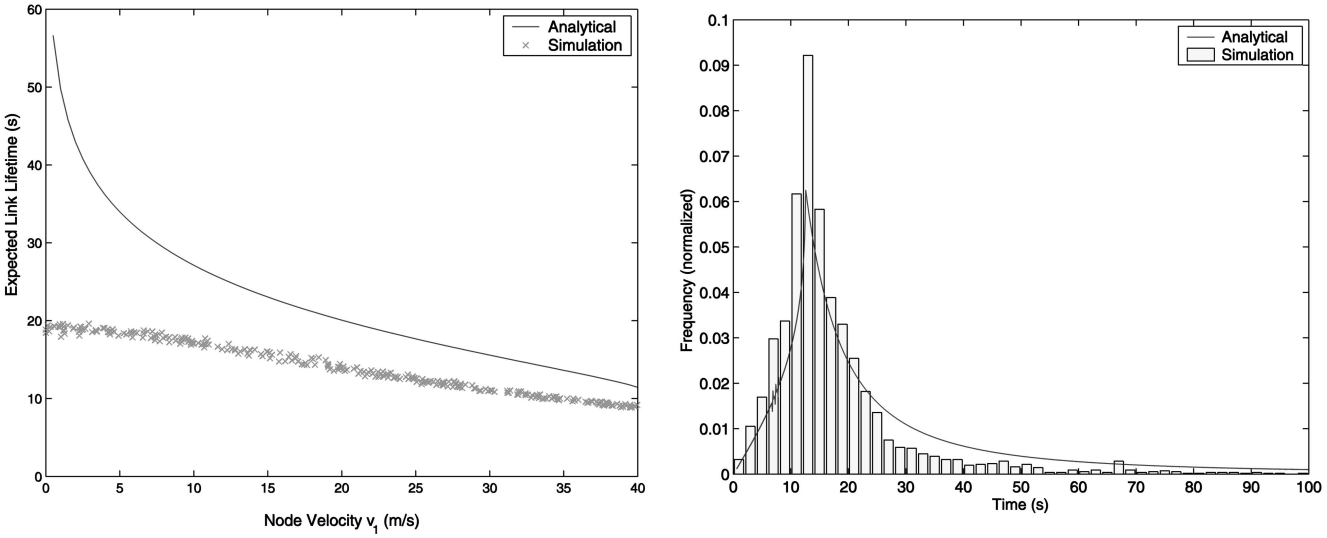

(a) (b)

Fig. 11. Comparison with simulation statistics: (a) expected link lifetime and (b) link lifetime PDF for a node with velocity $v_1 = 0\ m/s$.

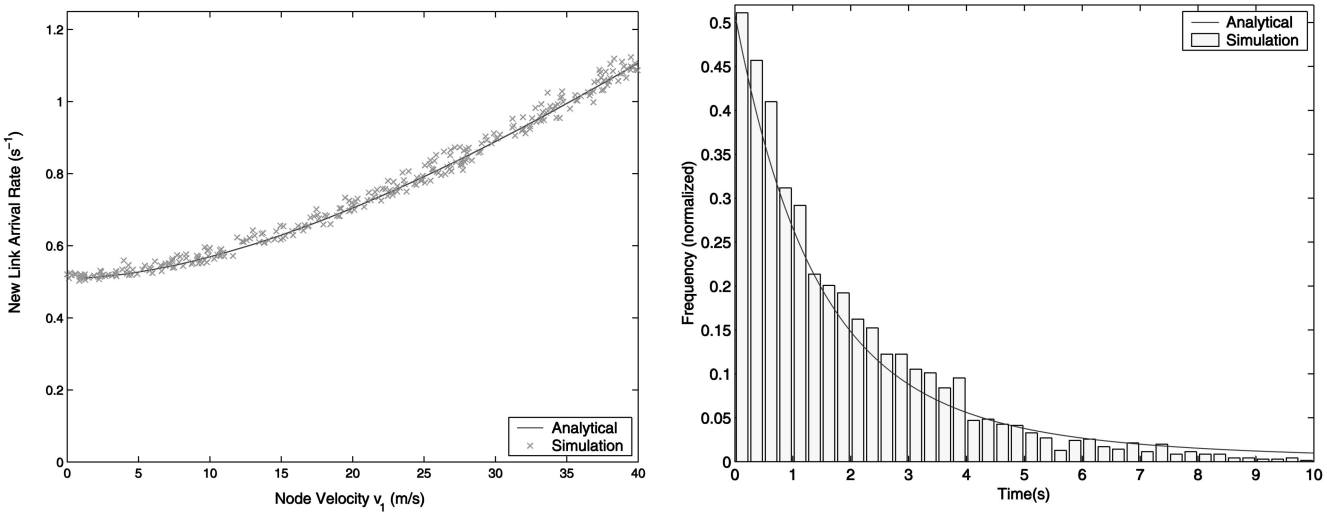

(a) (b)

Fig. 12. Comparison with simulation statistics: (a) expected new link arrival rate and (b) new link interarrival time PDF for a node with velocity $v_1 = 0\ m/s$.

5 Applying Link Dynamics Models in Protocol Design

The characterization of link dynamics gives us a formal understanding of their behavior in a mobile, multihop environment. The framework developed in Section 3 can form the basis for analyzing performance bounds of protocols in mobile ad hoc and sensor networks. Further, it can be used to design new algorithms enabling efficient communication in such networks. We discuss some representative applications of the framework below.

The link lifetime distribution can be used to determine the stability of links in the network. Once communication starts over a link, its residual lifetime distribution can be calculated as a function of the link lifetime distribution. Mathematically, the probability density $r_T^{v_1}(t)$ of residual link lifetime given that the link has been in existence for T seconds already can be expressed as

$$r_T^{v_1}(t) = \frac{f_{link}^{v_1}(t+T)}{1 - F_{link}^{v_1}(T)}. \tag{36}$$

Here, $f_{link}^{v_1}(\cdot)$ and $F_{link}^{v_1}(\cdot)$ are the link lifetime PDF and CDF, respectively, as derived in Section 3.2.

The residual link lifetime density can be used to evaluate the lifetime of a route in the network. For example, consider a route with K links and let $\mathbf{X_1}, \mathbf{X_2}, \cdots, \mathbf{X_K}$ be the random variables representing each of their residual lifetimes at the time when the route is formed, given that the links have already been in existence for $T_1, T_2, \cdots, T_K$ seconds, respectively. Let $\mathbf{Y}$ be a random variable representing the lifetime of the route formed by the K links. As the route is deemed to have failed when any of the K links breaks, the route

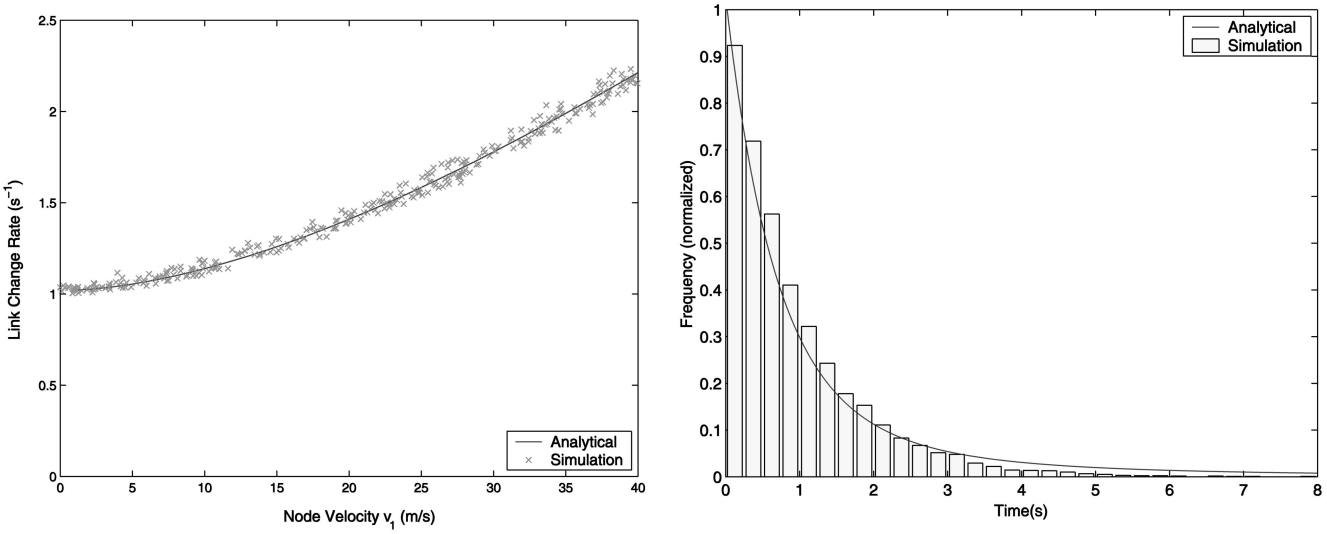

(a) (b)

Fig. 13. Comparison with simulation statistics: (a) expected link change rate and (b) link change interarrival time PDF for a node with velocity $v_1 = 0\ m/s$.

lifetime can be expressed as the minimum of the lifetimes of its constituent links.

$$\mathbf{Y} = min(\mathbf{X_1}, \mathbf{X_2}, \cdots, \mathbf{X_K}). \tag{37}$$

If we assume that the residual link lifetimes are independent, then the distribution $F_Y(t)$ of $\mathbf{Y}$ can be calculated as

$$\begin{aligned} F_Y(t) &= Prob\{\mathbf{Y} \le t\} \\ &= 1 - Prob\{min(\mathbf{X_1}, \mathbf{X_2}, \cdots, \mathbf{X_K}) > t\} \\ &= 1 - Prob\{\mathbf{X_1} > t\} \cdot Prob\{\mathbf{X_2} > t\} \cdots Prob\{\mathbf{X_K} > t\} \\ &= 1 - \Big[\big(1 - R_{T_1}^{v_{1_1}}(t)\big) \cdot \big(1 - R_{T_2}^{v_{1_2}}(t)\big) \cdots \big(1 - R_{T_K}^{v_{1_K}}(t)\big)\Big], \end{aligned} \tag{38}$$

where $R_{T_i}^{v_{1_i}}(t)$ is the cumulative distribution function of the residual link lifetime of the ith link in the route, whose upstream node is moving with velocity v_{1_i}, given that the link was formed T_i seconds ago. $R_{T_i}^{v_{1_i}}(t)$ can be evaluated by integrating the corresponding density as expressed in (36).

The route lifetime distribution can be used to analyze the performance of reactive and hybrid routing protocols in ad hoc and sensor networks. It can also be used to provide Quality of Service (QoS) in the network. For instance, the above framework can form the basis of schemes for selection of the most suitable set of routes for QoS techniques like Multipath routing [24] and Alternate Path Routing [26].

The performance of TCP in ad hoc networks is bottlenecked by its inability to adapt to link failures induced by mobility [14]. The route lifetime distribution can serve as a starting point for the estimation of the round-trip-time distribution between a source and a destination for a particular session. This could then be utilized to optimize the performance of TCP in mobile ad hoc networks.

The framework can be applied to design a strategy for optimal selection of the Time-to-Live (TTL) interval of route caches in on-demand routing protocols. For example, the work in [19] can be supplemented using the derived distributions in this paper to minimize the expected routing delay. It is also possible to develop alternate schemes to optimize other network performance metrics, if so desired.

Many protocols for mobile ad hoc and sensor networks employ a periodic beaconing (or "HELLO") mechanism as a means for neighbor discovery. The rate of link changes could be used to determine both the rate at which a node should broadcast these beacons and the corresponding timeout for declaring the loss of an existing neighbor.

Renewal theory [25] can be used to characterize the residual time w to arrival of the next link change after a given fixed instant t_0. Fig. 14 shows the time-line where t_0 and w are indicated and the "x"-es represent the arrival of link changes. The probability density of the residual time $f_w^{v_1}(w)$ of w is given by

$$f_w^{v_1}(w) = \dot{\gamma}(v_1)\big[1 - F_{change}^{v_1}(w)\big], \tag{39}$$

where $\dot{\gamma}(v_1)$ and $F_{change}^{v_1}(w)$ are the expected link change arrival rate and the link change interarrival time distribution, respectively, as found before. Similarly, given a fixed point t_0, the density of the residual time to arrival of the next new link or the next link breakage can be calculated by appropriately replacing the corresponding functions in (39).

Topology control and management is another area which could benefit from the developed framework. The framework provides relationships between various network characteristics like transmission range, node density, node

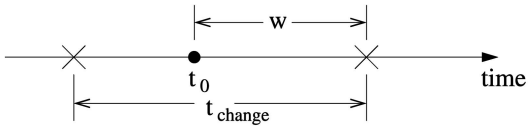

Fig. 14. Time-line where the "x"-es represent the arrival of link changes and t_0 is a fixed point.

velocity, link lifetime, link changes, and number of neighbors. These relationships could be used to form simple rules of thumb for topology control or more sophisticated schemes could be designed using them as the basis.

The framework can also serve as the basis for designing a scheme that determines each node's optimal zone radius in the Independent Zone Routing (IZR) framework [31], a hybrid adaptive routing framework for mobile ad hoc networks.

Although the node behavior in certain real-world environments may be different from how it is modeled here, the framework can still serve to provide an indication of the bounds on network performance. Further, the methodology adopted could be extended to analyze link dynamics under different assumptions on node behavior as well. For example, for a network where a certain fraction of the nodes is stationary, the probability density $f^{v_1}_{combined}(t)$ of link lifetime for a node moving with velocity v_1 can be expressed as

$$f^{v_1}_{combined}(t) = (1 - p_{stat}) \cdot f^{v_1}_{moving}(t) + p_{stat} \cdot f^{v_1}_{stat}(t), \qquad (40)$$

where p_{stat} is the probability that a node is stationary, $f^{v_1}_{moving}(t)$ is the probability density function of link lifetime as derived in Section 3, and $f^{v_1}_{stat}(t)$ is the probability density function of link lifetime when the rest of the nodes in the network are stationary. It is easy to derive $f^{v_1}_{stat}(t)$ along the same lines as $f^{v_1}_{moving}(t)$.

Another interesting application of the analytical framework is the design of an efficient strategy for proactive protocols to broadcast routing updates in the network. We focus on this particular application in the next section in order to provide an illustration of the framework's applicability.

6 Proactive Updating

Proactive or *table-driven* routing protocols for ad hoc networks maintain routes to all the nodes in the network at all times so that, when a data packet needs to be forwarded, a route is known and can immediately be used. This is done by regular broadcast of routing updates reflecting changes in the network topology into the network. Examples of proactive routing protocols include DSDV [28], TBRPF [2], OLSR [6], WRP [23], STAR [8], and FSR [27]. Hybrid routing approaches like ZRP [11] also utilize a limited-scope proactive protocol as one of its components [12].

The performance of a proactive protocol depends on the particular scheme the protocol uses to broadcast the link-state or the distance-vector updates to other nodes in the network. If these updates are broadcasted too often, it may lead to wastage of resources and inefficient performance of the network. On the other hand, if these updates are broadcast too infrequently, nodes may maintain an incorrect picture of the network, leading to lost packets and routing loops.

In the following, we develop a strategy for broadcasting of routing updates by proactive protocols using the developed framework. The goal of the strategy is to reduce the amount of routing overhead in the network, while ensuring that the performance of the network does not deteriorate. This would improve the efficiency and scalability of proactive (as well as hybrid) protocols, making them better suited for the dynamic ad hoc networking environment.

6.1 Background and Motivation

All proactive routing protocols utilize periodic beacons as a means for Neighbor Discovery—that is, to detect the presence of a new node within the transmission zone or a loss of a link to an existing neighbor. The periodic beacons are transmitted at a higher frequency than the proactive updates and provide information that is used as an input to proactive updating and to refresh the local routing tables.

Some of the proactive protocols broadcast routing updates *periodically* with a fixed interval. Examples include the DARPA packet-radio network project [17], the Intrazone Routing Protocol (IARP) component of the Zone Routing framework [11], and Fisheye State Routing (FSR) [27]. Other proactive routing protocols broadcast an update for *each detected change* in the link status. Protocols based on this approach include Destination Sequenced Distance Vector (DSDV) Routing [28], Wireless Routing Protocol (WRP) [23], Source Tree Adaptive Routing (STAR) [8], and Topology Broadcast based on Reverse Path Forwarding (TBRPF) [2].

Broadcasting a routing update each time a change is detected has the potential of producing a lot of control traffic. One reason is that, in a wireless environment, the radio link between mobile nodes may experience frequent disconnects and reconnects. Also, often, a node's link changes may arrive quite closely spaced in time. For example, if a node starts moving all of a sudden, its links may break or new links may be created in quick succession. Thus, instead of broadcasting an update for each of the detected changes, if the node were to wait for a small amount of time before it broadcast the next update, information about many changes can be conveyed in a single update packet. Hence, the node would save by broadcasting a considerably smaller number of update packets, provided that a small delay can be tolerated by the network.

Consequently, broadcasting proactive updates involves a trade-off between the amount of control traffic overhead and the consistency of the network topology information maintained by the nodes. Periodic updates are sometimes preferred in proactive protocols as they aggregate the information about link changes during the last interval in a single packet. However, broadcasting periodic updates at fixed intervals also has its own problems. Usually, the update interval is designed to reduce the delay in the worst-case scenario—enabling the updates of the nodes with the most frequent link changes[3] to be obtained on time by other nodes [11]. Thus, the nodes which are experiencing much less frequent changes end up broadcasting a lot of redundant updates, which could be saved if a velocity-sensitive scheme were to be used.

3. The dependence of link change rate on node velocity is plotted in Fig. 7.

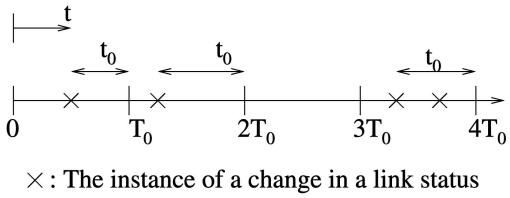

Fig. 15. Time-line showing the periodic updates after every interval T_0, the arrival of link changes, and the residual time t_0 to the next link-state broadcast after the arrival of a link change.

With an aim of studying and optimizing the trade-off between aggregation of multiple link change updates in a single packet and the delay involved in dissemination of information about these link changes, we design a proactive updating strategy in the next section.

6.2 Updating Strategy Design

With an aim of reducing the routing overhead, we wish to find the largest update period for periodically broadcasting routing updates such that the expected delay between the detection of a link change and the next broadcast of the routing update is still "small" enough. In Fig. 15, each T_0 period represents the update interval, the "x"-es represent detection of a link change, and t_0 is the delay experienced by the first link change during an update interval before the corresponding update is broadcasted.

The problem statement can thus be formulated as follows: Maximize the period T_0 such that the average waiting time for the broadcast of the *first* link change during an update interval is bounded. In other words, *maximize* T_0 *such that* $E(t_0) \leq \alpha$, where α is the bound required on the mean value of the delay with which the update about the first detected change in an update interval is broadcast. α could be considered a Quality of Service parameter for the network performance. Thus, the delay before which a topology change in the network can be reflected in the routing tables of other nodes is dependent on α.

As justified in Section 3.7, the link change interarrival time density for a node can be modeled by an exponential function. Therefore, the link change interarrival time density for a node can be stated as $f_{change}(t) = \lambda e^{-\lambda t}$. Here, λ represents the mean link change rate for a node and is a function of its velocity.

With the end of the last update interval as reference, let t indicate the time at which the next link change is detected by a particular node. Define $\eta = \lceil \frac{t}{T_0} \rceil$ be to the interval number in which the next link change is detected following the last update. Let $\theta = \eta T_0 - t$. Hence, $\theta \in [0, T_0]$. The cumulative distribution function for the random variable θ is given by

$$\begin{aligned} &Prob(\theta \leq t_0) \\ &= Prob\Big(t \in \big\{[T_0 - t_0, T_0] \cup [2T_0 - t_0, 2T_0] \cup [3T_0 - t_0, 3T_0] \cup \cdots\big\}\Big) \\ &= \sum_{k=1}^{\infty} (e^{-\lambda(kT_0 - t_0)} - e^{-\lambda k T_0}) = \frac{e^{-\lambda T_0}}{1 - e^{-\lambda T_0}} (e^{\lambda t_0} - 1). \end{aligned} \tag{41}$$

The probability density function of θ can be found by differentiating (41).

$$f_\theta(t_0) = \frac{e^{-\lambda T_0}}{1 - e^{-\lambda T_0}} \lambda e^{\lambda t_0} \qquad 0 \leq t_0 \leq T_0. \tag{42}$$

Therefore, the expected value of θ (or, equivalently, t_0 in Fig. 15) is given by

$$\begin{aligned} E(t_0) &= \frac{e^{-\lambda T_0}}{1 - e^{-\lambda T_0}} \lambda \int_0^{T_0} t' e^{\lambda t'} dt' \\ \Rightarrow E(t_0) &= \frac{T_0}{1 - e^{-\lambda T_0}} - \frac{1}{\lambda} \leq \alpha. \end{aligned} \tag{43}$$

As λ represents the mean link change rate for a node, it can be calculated using (28) if the node velocity is known.[4] Alternately, a node can simply estimate it online by measuring the rate of changes in its set of links, averaged over a window. Such an online estimate has the advantage that it would adapt to any changes in the node mobility.

Equation (43) provides us with a strategy for broadcasting the routing updates in the network. Given the value of the bound α and the adaptively estimated link change arrival rate λ, the maximum value of T_0 which satisfies (43) is calculated at the start of an update interval. If at least one link change is detected during the update interval, a routing update is broadcast. If no link changes are detected, no update is broadcast, reducing the overhead. Additionally, an update is broadcast if the node has not broadcast any updates in the last MAX_IDLE_SLOTS intervals. Broadcasting an update at least every MAX_IDLE_SLOTS is used as a protection against transmission errors and loss of soft state.

Note that this strategy determines the generation of a new update by a node. The nodes receiving the broadcast update would still need to forward them in the network according to the rules of the particular proactive protocol being used.

6.3 Performance Evaluation

The performance of the derived strategy is evaluated using simulations. A link-state-based proactive routing protocol, as described in [12], is utilized. The network consists of 50 nodes spread randomly in a square of side $990.8\ meters$. The transmission radius of the nodes is set to $R = 250\ meters$ so that the node density turns out to be $\sigma = \frac{10}{\pi R^2}$. A node moves at a constant speed v which is chosen from a uniform distribution between $a = 0\ meters/second$ and $b = 40\ meters/second$. It is assigned an initial direction θ, which is uniformly distributed between 0 and 2π. When a node reaches an edge of the simulation region, it is reflected back into the network such that the angle of incidence equals the angle of reflection (*billiard mobility* model). Each node initiates a session with a randomly chosen destination node and sends an average of five packets. The number of packets in a particular session is *Poisson* distributed and the interarrival delay between sessions for a particular node is exponentially distributed with a mean of $2.5\ seconds$. The simulation duration is set to $300\ seconds$. The traces for mobility and session statistics were kept the same for

4. As may be provided, for example, by GPS.

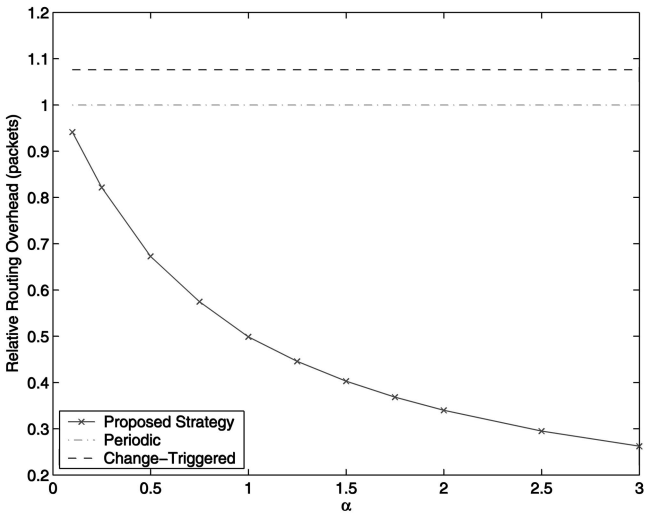

Fig. 16. Total routing overhead (packets) relative to Periodic updating as a function of the bound α.

different simulation runs. The simulations have been performed in the $OPNET$® network simulation environment. No data was collected for the first 5 seconds to allow the route discovery process to stabilize. The parameter MAX_IDLE_SLOTS was set to 50 for the simulations.

The proposed strategy is compared to the two commonly used updating schemes in existing proactive protocols, as described in Section 6.1.

1. **Change-Triggered**. A node broadcasts an update whenever a link change is detected. If no broadcasts have been made in the last
$$BROADCAST\_TIMEOUT = 5\ seconds,$$
the node broadcasts an update.
2. **Periodic**. All nodes broadcast their link-states every $T_{periodic}$ seconds. This period is computed using $T_{periodic} = \frac{3R/20}{v_m}$ [11], where v_m is the maximum velocity of the nodes in the network and R is the transmission radius.

Fig. 16 plots the total routing overhead generated in the network for the proposed strategy as a function of the parameter α that bounds the mean delay involved in broadcasting a routing update. The routing overhead is measured in terms of the number of packets transmitted and is shown relative to the overhead associated with the Periodic updating scheme. As can be observed from the figure, the proposed strategy leads to considerable reduction in the routing overhead as compared to the Periodic or the Change-Triggered schemes, especially for values of $\alpha \geq 0.5$. Reduction in control traffic overhead for a routing protocol is an important goal as it translates to lower power consumption, less congestion, reduced memory and processing requirements, and easier access to the communication channel. This increases the efficiency and scalability of the protocol.

Fig. 17a shows that the fraction of data packets delivered to the destination remains high for the values of α considered. At the same time, the delay involved in delivering the data packets to the destination increases as α is increased, as observed from Fig. 17b. These effects are due to the high amount of redundancy in routing information maintained by a link-state routing protocol. As each node has complete topology information about the network, when a data packet reaches a node whose next forwarding link is broken, it is usually able to find an alternate path to the destination.[5] Note that, as indicated in Section 6.1, the periodic beaconing mechanism is able to provide up-to-date information about the status of a node's links with its immediate neighbors in advance, which is used to preemptively find an alternate path if the next forwarding link is broken. Thus, the data packet delivery fraction remains high even for larger values of α. However, larger values of α imply that the nodes may have more stale global routing information,[6] increasing the likelihood of the data packets encountering nodes whose next forwarding link is broken. This leads to the data packets possibly being rerouted along alternate paths, increasing the effective path length, and thus increasing the latency.

Hence, considerable reduction in routing overhead can be obtained by choosing an appropriate value of α depending on the quality of service needed from the network. For example, setting $\alpha = 1$ reduces the routing overhead by more than 50 percent as compared to Periodic or Change-Triggered updating, while keeping the data packet delivery fraction high and increasing the data packet delay only marginally. For $\alpha = 0.5$, the reduction in routing overhead is more than 33 percent (as compared to Periodic or Change-Triggered updating), the data packet delay also reduces and the data packet delivery fraction remains high. Even bigger savings in routing overhead can be obtained if some latency can be tolerated by the application layer.

Such an updating strategy can be used by a purely proactive routing protocol without introducing any additional complexity. Alternately, it can be used by the proactive component of hybrid approaches like the Zone Routing Protocol (ZRP) [13] or its adaptive version, the Independent Zone Routing (IZR) framework [31]. This would further increase their scalability by limiting the updating to the local neighborhood.

7 Conclusions

In this paper, we have addressed the general problem of mobility in energy-constrained wireless ad hoc and sensor networks. In such situations, communication links pass into and out of existence as nodes move toward and away from one another. That such varying connectivity has an impact on network performance is intuitively clear; in this paper, we showed that a detailed analytical model for time-varying connectivity can be derived and incorporated into the process of protocol design, with significant positive effect.

A number of applications for our analytic framework were considered, including the design of protocols for

5. Assuming that the network is fairly well-connected.
6. Even though the information about the status of the links to its immediate neighbors is still fresh, thanks to the periodic beaconing mechanism.

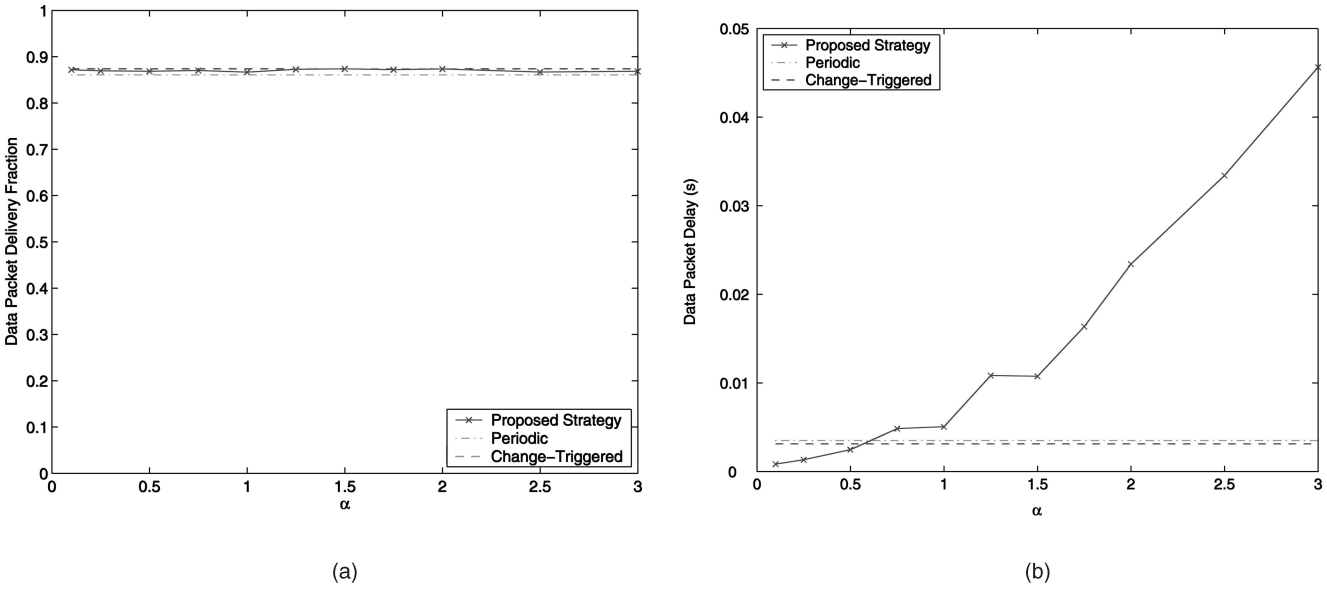

(a) (b)

Fig. 17. (a) Data packet delivery fraction. (b) Data packet delivery delay as a function of the bound α.

transport control, routing, medium access, Quality of Service (QoS), and topology control. As a detailed example, we designed an efficient updating strategy for proactive routing protocols. We showed that the strategy can lead to substantial performance improvements in terms of reduction in routing overhead, while maintaining high data packet delivery ratio and acceptable latency.

APPENDIX

JOINT PROBABILITY DENSITY OF v, ϕ, AND α

Here, we derive the joint probability density function $f_{v\phi\alpha}(v,\phi,\alpha)$ for the nodes that enter the transmission zone of node 1, as illustrated in Fig. 1. Now,

$$f_{v\phi\alpha}(v,\phi,\alpha) = f_{\alpha|v\phi}(\alpha|v,\phi) f_{v\phi}(v,\phi). \tag{44}$$

$f_{\alpha|v\phi}(\alpha|v,\phi)$ is the conditional probability density function of the angle α defining node 2's point of entry ($-R\cos\alpha$, $R\sin\alpha$) into the transmission zone of node 1, given its relative velocity $\vec{v} = v\cos\phi\hat{i} + v\sin\phi\hat{j}$.[7] Now, given the direction ϕ of node 2's relative velocity, the node can only enter the transmission zone from a point on the semicircle $\alpha \in I_0 = [-(\frac{\pi}{2}+\phi), \frac{\pi}{2}-\phi]$. Consider the diameter of this semicircle, which is perpendicular to the direction of node 2's relative velocity. As nodes in the network are assumed to be uniformly distributed, a node entering the zone with velocity $\vec{v}$ can intersect this diameter at any point on it with equal probability. This is illustrated in Fig. 18a, where the node's trajectory is equally likely to intersect the diameter QR at any point $Q, P1, P2, \cdots, R$ on it, indicating that the probability of location of this point of intersection is uniformly distributed on the diameter.

In Fig. 18b, node 2 enters the transmission zone at T and travels along TV, which makes an angle ϕ with the horizontal. OT makes an angle α with OX''. QR is the diameter perpendicular to TV, defining the semicircle $\alpha \in I_0$. Let OS = r, where S is the point of intersection of TV and QR. As OT = OV = R, it is easy to see that $r = R\sin(\alpha+\phi)$.

Let $\boldsymbol{\alpha}$ be the random variable representing the angle defining the point of entry of node 2 in the zone. For $\alpha \in I_0$, the conditional distribution function of α is

$$\begin{aligned} F_{\alpha|v\phi}(\alpha|v,\phi) &= Prob\{\boldsymbol{\alpha} \le \alpha | v,\phi\} \\ &= \int_{-R}^{r} \frac{1}{2R} dr \\ &= \frac{1}{2}(1+\sin(\alpha+\phi)). \end{aligned} \tag{45}$$

Hence, by differentiating (45),

$$\begin{aligned} f_{\alpha|v\phi}(\alpha|v,\phi) &= \begin{cases} \frac{1}{2}\cos(\alpha+\phi) & \alpha \in I_0 \\ 0 & otherwise \end{cases} \\ &= \frac{1}{2}\cos(\alpha+\phi)\left\{ u\Big(\alpha + \big(\frac{\pi}{2}+\phi\big)\Big) - u\Big(\alpha - \big(\frac{\pi}{2}-\phi\big)\Big)\right\}, \end{aligned} \tag{46}$$

where $u(\cdot)$ is the standard unit step function. Note that, for $\alpha \in I_0$, $\cos(\alpha+\phi) \ge 0\ \forall\phi \in [-\pi,\pi]$.

$f_{v\phi}(v,\phi)$ is the joint probability density function of v and ϕ for the nodes that enter the zone. This is simply the density of the relative velocity $\vec{v}$ of the nodes in the network. It can be calculated by

$$f_{v\phi}(v,\phi) = \frac{f_{v_2\theta}(v_2^*,\theta^*)}{|J(v_2^*,\theta^*)|}, \tag{47}$$

where $f_{v_2\theta}(v_2^*,\theta^*)$ is the joint PDF of v_2 and θ, v_2^* and θ^* are the values of v_2 and θ that satisfy (3) and (4), and

$$J(v_2,\theta) = \begin{vmatrix} \frac{\partial v}{\partial v_2} & \frac{\partial v}{\partial \theta} \\ \frac{\partial \phi}{\partial v_2} & \frac{\partial \phi}{\partial \theta} \end{vmatrix} \tag{48}$$

is the *Jacobian* for the transformation.

7. Note that α is measured clockwise from the negative X axis.

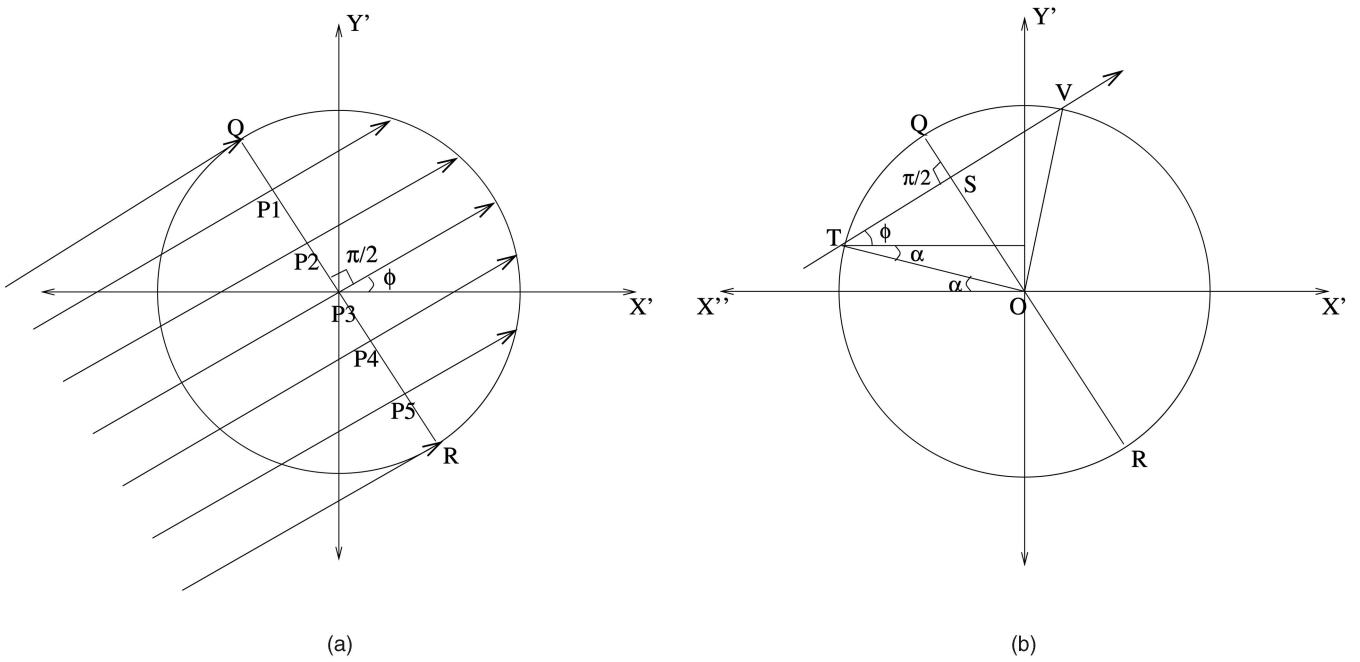

Fig. 18. (a) Given the direction of a node's relative velocity, it can intersect the diameter QR at any point on it with equal probability. (b) Calculation of $f_{\alpha|v\phi}(\alpha|v,\phi)$.

Solving (3) and (4) for v_2^* and θ^* gives

$$\theta^* = \tan^{-1}\Big(\frac{\sin\phi}{\cos\phi + v_1/v}\Big), \tag{49}$$

$$v_2^* = \sqrt{v^2 + v_1^2 + 2vv_1\cos\phi}. \tag{50}$$

Using (3) and (4) to get the derivatives for the *Jacobian*,

$$J(v_2,\theta) = \begin{vmatrix} \frac{v_2 - v_1\cos\theta}{\sqrt{v_1^2+v_2^2-2v_1v_2\cos\theta}} & \frac{v_1v_2\sin\theta}{\sqrt{v_1^2+v_2^2-2v_1v_2\cos\theta}} \\ \frac{-v_1\sin\theta}{v_1^2+v_2^2-2v_1v_2\cos\theta} & \frac{v_2^2-v_1v_2\cos\theta}{v_1^2+v_2^2-2v_1v_2\cos\theta} \end{vmatrix} \tag{51}$$

$$= \frac{v_2}{\sqrt{v_1^2+v_2^2-2v_1v_2\cos\theta}}.$$

From Assumption 2, v_2 is uniformly distributed between a and b. Also, from Assumption 3, θ is uniformly distributed between 0 and 2π. Thus, their individual probability density functions are given by

$$f_{v_2}(v_2) = \frac{1}{b-a}\Big\{u(v_2-a) - u(v_2-b)\Big\}, \tag{52}$$

$$f_\theta(\theta) = \frac{1}{2\pi}. \tag{53}$$

As v_2 and θ are assumed to be independent (Assumption 4), their joint probability density function is simply the product of their individual density functions:

$$f_{v_2\theta}(v_2,\theta) = \frac{1}{2\pi(b-a)}\Big\{u(v_2-a) - u(v_2-b)\Big\}. \tag{54}$$

Therefore, from (47), (54), (51), (49), and (50), we get

$$f_{v\phi}(v,\phi) = \frac{1}{2\pi(b-a)}vg(v,\phi,v_1), \tag{55}$$

where $g(v,\phi,v_1)$ is as defined in (16).

Hence, the joint density of v, ϕ, and α can be expressed as the product of (46) and (55):

$$f_{v\phi\alpha}(v,\phi,\alpha) = \frac{1}{4\pi(b-a)}v\cos(\alpha+\phi)g(v,\phi,v_1) \Big\{u\big(\alpha+(\frac{\pi}{2}+\phi)\big) - u\big(\alpha-(\frac{\pi}{2}-\phi)\big)\Big\}. \tag{56}$$

ACKNOWLEDGMENTS

S.B. Wicker is supported in part by the US National Science Foundation ITR and Nets-NOSS programs and the US Office of Naval Research MURI program.

REFERENCES

[1] S. Agarwal, A. Ahuja, J.P. Singh, and R. Shorey, "Route-Lifetime Assessment Based Routing (RABR) Protocol for Mobile Ad-Hoc Networks," *Proc. IEEE Int'l Conf. Computers,* vol. 3, pp. 1697-1701, 2000.

[2] B. Bellur and R.G. Ogier, "A Reliable, Efficient Topology Broadcast Protocol for Dynamic Networks," *Proc. IEEE Infocom Conf.,* Mar. 1999.

[3] C. Bettstetter, H. Hartenstein, and X. Perez-Costa, "Stochastic Properties of the Random Waypoint Mobility Model," *ACM/ Kluwer Wireless Networks,* special issue on modeling and analysis of mobile networks, 2004.

[4] C. Bettstetter, G. Resta, and P. Santi, "The Node Distribution of the Random Waypoint Mobility Model for Wireless Ad Hoc Networks," *IEEE Trans. Mobile Computing,* vol. 2, no. 3, pp. 257-269, July-Sept. 2003.

[5] T. Camp, J. Boleng, and V. Davies, "A Survey of Mobility Models for Ad Hoc Network Research," *Wireless Comm. and Mobile Computing (WCMC),* vol. 2, no. 5, pp. 483-502, 2002.

[6] T. Clausen et al., "Optimized Link State Routing Protocol (OLSR)," *IETF MANET,* Internet Draft, Oct. 2001.

[7] R. Dube, C. Rais, K.-Y. Wang, and S. Tripathi, "Signal Stability Based Adaptive Routing (SSA) for Ad Hoc Networks," *IEEE Personal Comm.,* pp. 36-45, Feb. 1997.

[8] J.J. Garcia-Luna-Aceves and M. Spohn, "Efficient Routing in Packet-Radio Networks Using Link-State Information," *Proc. IEEE Wireless Comm. and Networking Conf. (WCNC '99),* Aug. 1999.

[9] M. Gerharz, C. de Waal,, M. Frank, and P. Martini, "Link Stability in Mobile Wireless Ad Hoc Networks," *Proc. IEEE Conf. Local Computer Networks,* Nov. 2002.
[10] A.J. Goldsmith and S.B. Wicker, "Design Challenges for Energy-Constrained Ad Hoc Wireless Networks," *IEEE Wireless Comm.,* vol. 9, no. 4, pp. 8-27 Aug. 2002.
[11] Z.J. Haas and M.R. Pearlman, "The Performance of Query Control Schemes for the Zone Routing Protocol," *ACM/IEEE Trans. Networking,* vol. 9, no. 4, pp. 427-438, Aug. 2001.
[12] Z.J. Haas, M.R. Pearlman, and P. Samar, "The Intrazone Routing Protocol (IARP) for Ad Hoc Networks," *IETF MANET,* Internet Draft, July 2002.
[13] Z.J. Haas, M.R. Pearlman, and P. Samar, "The Zone Routing Protocol (ZRP) for Ad Hoc Networks," *IETF MANET,* Internet Draft, July 2002.
[14] G.D. Holland and N.H. Vaidya, "Analysis of TCP Performance over Mobile Ad Hoc Networks," *Proc. MobiCom Conf.,* Aug. 1999.
[15] Y.-C. Hu and D.B. Johnson, "Caching Strategies in On-Demand Routing Protocols for Wireless Ad Hoc Networks," *Proc. MobiCom Conf.,* Aug. 2000.
[16] S. Jiang, D.J. He, and J.Q. Rao, "A Prediction-Based Link Availability Estimation for Mobile Ad Hoc Networks," *Proc. IEEE Infocom Conf.,* Apr. 2001.
[17] J. Jubin and J. Tornow, "The DARPA Packet Radio Network Protocols," *Proc. IEEE,* vol. 75, no. 1, Jan. 1987.
[18] J.F.C. Kingman, *Poisson Processes,* vol. 3. New York: Oxford Univ. Press, 1993.
[19] B. Liang and Z.J. Haas, "Optimizing Route-Cache Lifetime in Ad Hoc Networks," *Proc. IEEE Infocom Conf.,* Apr. 2003.
[20] G. Lim, K. Shin, S. Lee, H. Yoon, and J.S. Ma, "Link Stability and Route Lifetime in Ad Hoc Wireless Networks," *Proc. 2002 Int'l Conf. Parallel Processing Workshops (ICPPW '02),* Aug. 2002.
[21] A.B. McDonald and T.F. Znati, "A Mobility-Based Framework for Adaptive Clustering in Wireless Ad Hoc Networks," *IEEE J. Selected Areas in Comm.,* vol. 17, no. 8, pp. 1466-1487, Aug. 1999.
[22] J.P. Mullen, "Robust Approximations to the Distribution of Link Distances in a Wireless Network Occupying a Rectangular Region," *Mobile Computing and Comm. Rev.,* vol. 7, no. 2, Apr. 2003.
[23] S. Murthy and G. Luna-Aceves, "An Efficient Routing Protocol for Wireless Networks," *Mobile Networks and Applications,* vol. 1, no. 2, pp. 183-197, 1996.
[24] P. Papadimitratos, Z.J. Haas, and E.G. Sirer, "Path Set Selection in Mobile Ad Hoc Networks," *Proc. ACM MobiHoc Conf.,* June 2002.
[25] A. Papoulis, *Probability, Random Variables, and Stochastic Processes,* third ed. McGraw-Hill, 1991.
[26] M.R. Pearlman, Z.J. Haas, P. Scholander, and S.S. Tabrizi, "On the Impact of Alternate Path Routing for Load Balancing in Mobile Ad Hoc Networks," *Proc. ACM MobiHoc Conf.,* Aug. 2000.
[27] G. Pei, M. Gerla, and T.-W. Chen, "Fisheye State Routing: A Routing Scheme for Ad Hoc Wireless Networks," *Proc. Int'l Conf. Comm.,* June 2000.
[28] C. Perkins and P. Bhagwat, "Highly Dynamic Destination-Sequenced Distance-Vector Routing (DSDV) for Mobile Computers," *Proc. ACM SIGCOMM Conf.,* Oct. 1994.
[29] N. Sadagopan, F. Bai, B. Krishnamachari, and A. Helmy, "PATHS: Analysis of PATH Duration Statistics and Their Impact on Reactive MANET Routing Protocols," *Proc. MobiHoc Conf.,* June 2003.
[30] P. Samar, "Optimizing Protocols for Mobility in MultiHop Networks," PhD dissertation, Cornell Univ., 2004.
[31] P. Samar, M.R. Pearlman, and Z.J. Haas, "Independent Zone Routing: An Adaptive Hybrid Routing Framework for Ad Hoc Wireless Networks," *IEEE/ACM Trans. Networking,* vol. 12, no. 4, pp. 595-608, Aug. 2004.
[32] P. Samar and S.B. Wicker, "On the Behavior of Communication Links of a Node in a Multi-Hop Mobile Environment," *Proc. Fifth ACM Int'l Symp. Mobile Ad Hoc Networking and Computing (MobiHoc),* May 2004.
[33] W. Su, S.-J. Lee, and M. Gerla, "Mobility Prediction and Routing in Ad Hoc Wireless Networks," *Int'l J. Network Management,* vol. 11, no. 1, pp. 3-30, Jan./Feb. 2001.
[34] C.-K. Toh, "Associativity-Based Routing for Ad Hoc Networks," *Wireless Personal Comm.,* pp. 103-139, Mar. 1997.
[35] Y.-C. Tseng, Y.-F. Li, and Y.-C. Chang, "On Route Lifetime in Multihop Mobile Ad Hoc Networks," *IEEE Trans. Mobile Computing,* vol. 2, no. 4, Oct.-Dec. 2003.
[36] D. Turgut, S.K. Das, and M. Chatterjee, "Longevity of Routes in Mobile Ad Hoc Networks," *Proc. Vehicular Technology Conf.,* May 2001.
[37] E.W. Weisstein, "Torus," *MathWorld,* http://mathworld.wolfram.com/Torus.html, 2006.
[38] S.B. Wicker, *Error Control Systems for Digital Communication and Storage.* Prentice Hall, 1995.
[39] J. Yoon, M. Liu, and B. Noble, "Random Waypoint Considered Harmful," *Proc. IEEE INFOCOM Conf.,* Apr. 2003.

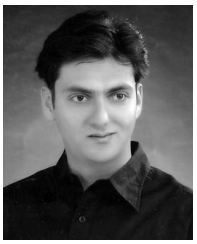

Prince Samar received the BTech degree in electrical engineering from the Indian Institute of Technology, Bombay, India, in 1999. He received the MS degree in 2003 and the PhD degree in 2004, both in electrical and computer engineering, from Cornell University, Ithaca, New York. He is currently working at Airvana Inc. on the design and development of mobile broadband network infrastructure. His interests are in the areas of wireless mobile systems and networking. His research has focused on the design of routing protocols, analysis of mobility, and performance optimization in ad hoc, sensor, and cellular networks.

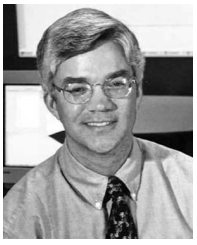

Stephen B. Wicker received the BSEE degree from the University of Virginia in 1982. He received the MSEE degree from Purdue University in 1983 and the PhD degree in electrical engineering from the University of Southern California in 1987. He is a professor of electrical and computer engineering at Cornell University. He is the author of *Codes, Graphs, and Iterative Decoding* (Kluwer, 2002), *Turbo Coding* (Kluwer, 1999), *Error Control Systems for Digital Communication and Storage* (Prentice Hall, 1995), and *Reed-Solomon Codes and Their Applications* (IEEE Press, 1994). He has served as an associate editor for coding theory and techniques for the *IEEE Transactions on Communications*, and has served two terms as a member of the Board of Governors of the IEEE Information Theory Society. Professor Wicker teaches and conducts research in wireless information networks, digital systems, self-configuring networks, and game theory. His current research focuses on the use of game theory in the development of highly distributed, adaptive networks. He was awarded the 1988 Cornell College of Engineering Michael Tien Teaching Award and the 2000 Cornell School of Electrical and Computer Engineering Teaching Award. He has served as a consultant in wireless telecommunications systems and digital systems for various companies and governments in North America, Europe, and Asia.